PHYSICAL REVIEW B **92**, 075420 (2015)

Entanglement creation in electron-electron collisions at solid surfaces

R. Feder,[1,2] F. Giebels,[1] and H. Gollisch[1]
[1]*Theoretische Festkörperphysik, Universität Duisburg-Essen, 47048 Duisburg, Germany*
[2]*Max-Planck Institut für Mikrostrukturphysik, Weinberg 2, 06120 Halle, Germany*

(Received 6 May 2015; published 17 August 2015)

For spin-polarized low-energy electrons impinging on a crystalline surface, an important reaction channel is the collision with a bound valence electron of opposite spin, followed by the emission of a correlated electron pair with antiparallel spins. While primary and valence electrons are not entangled, the screened Coulomb interaction generates spin entanglement between the two outgoing electrons. As a quantitative measure of this entanglement, we calculated a modified von Neumann entropy in terms of direct and exchange transition matrix elements. For coplanar symmetric setups with equal energies of antiparallel-spin electrons, maximal entanglement is analytically shown to occur quite universally, irrespective of the choice of the primary electron energy, the outgoing electron energy, and polar emission angle, and even of the choice of the surface system. Numerical results for Fe(110) and Cu(111) demonstrate first that strong entanglement can persist for unequal energies and second that an overall entanglement reduction due to nonentangled parallel-spin electrons can be avoided for ferromagnetic and even for nonmagnetic surfaces.

DOI: 10.1103/PhysRevB.92.075420 PACS number(s): 03.65.Nk, 03.67.Bg, 79.60.−i

I. INTRODUCTION

For systems involving two or more particles, entanglement of the wave function is a fundamental feature of quantum mechanics with counterintuitive consequences, which was seminally highlighted by the Einstein-Podolsky-Rosen (EPR) Gedanken experiment [1] and its discussion by Schrödinger [2]. Formally, entanglement means that the few- or many-particle wave function cannot be expressed as an appropriate product of single-particle wave functions (simple product in the case of distinguishable particles, antisymmetrized or symmetrized for identical fermions or bosons). The physical implication is that it is not possible to attribute a complete set of properties to each of the particles (cf., e.g., [3] and references therein). Entanglement and its central role in a variety of current research areas (like quantum cryptography, teleportation, and quantum computing) have since been the subject of a vast number of theoretical and experimental studies, for which it must suffice here to refer to a selection of review articles [4–8].

As regards the actual creation of entangled states, interaction between the particles, especially scattering, is a widely usable mechanism. Let two particles, which are initially far apart and not entangled, move towards each other and interact. After the collision, the two-particle wave function will in general be entangled. Such entanglement creation by interaction has been theoretically explored for pairs of distinguishable particles and for identical fermions within one-, two-, and three-dimensional models for various types of interaction (see, e.g., [9–16] and references therein).

A particularly transparent and instructive representative of entangled two-particle states is the spin-entangled state of two identical fermions, which was proposed in Bohm's version of the EPR paradox [17] and considered by Bell [18] as one of the paradigmatic states, which violate Bell's inequalities and exhibit nonlocal quantum correlations. This singlet state is hence also referred to as the first Bell state.

In principle, this state as well as less strongly spin-entangled two-fermion states can be created in the scattering of two free identical spin-one-half fermions via Coulomb interaction (cf. [19] and references therein). A detailed analysis of the post-collision two-fermion state and its spin entanglement as a function of the scattering angle has been given in [20]. Maximal spin entanglement is obtained if—in the laboratory system, with one fermion initially at rest—the scattering angle is 45°, for which the energy of each fermion is half the energy of the initially propagating fermion.

In the present paper we predict that electron pairs with maximal spin entanglement can be produced for a wider range of scattering angles and post-collision energies if a low-energy electron (with energy below about 100 eV) impinges on a crystalline surface, interacts via a screened Coulomb interaction with a bound-state electron, and both electrons subsequently exit from the surface and propagate over a macroscopic distance. The momentum-resolved coincident detection of such electron pairs, usually referred to as (e,2e) spectroscopy, has over the past two decades matured into a powerful source of information on electron-electron scattering dynamics as well as on exchange and Coulomb correlation between electrons in condensed matter ([21–27] and references therein). As regards the entanglement of these pairs, however, we are not aware of a theoretical study nor of an experimental demonstration. The former is the aim of the present work.

The paper is organized as follows. In Sec. II we outline a theoretical treatment of the (e,2e) process, yielding a formal expression for the post-collision two-electron state. In Sec. III the entanglement of this state is addressed and quantified by a modified von Neumann entropy. Subsequently we explore geometry and energy conditions, for which this entropy attains its maximal value. Our general analytical findings are then complemented by numerically calculated (e,2e) intensity and entanglement results for the ferromagnetic Fe(110) surface and for Cu(111). Some concluding remarks are made in Sec. IV.

II. THEORY OF ELECTRON-INDUCED TWO-ELECTRON EMISSION

In the following we recall key aspects of a previously developed (e,2e) formalism [21,28] and then focus on the states representing two outgoing electrons with either parallel or antiparallel spins. The formalism is based on the two-electron Hamiltonian

$$H = H_1 + H_2 + U, \tag{1}$$

where H_1 and H_2 are two one-electron Hamiltonians with an effective one-electron potential, which represents the interaction of each electron with the semi-infinite crystal or adsorbate system. The two-body potential U, which describes the interaction between the two electrons, is the bare Coulomb potential if both electrons are in the vacuum region between the surface and the detectors, and a screened Coulomb potential if at least one electron is inside the crystal.

In the framework of standard perturbation theory (cf. standard textbooks on quantum mechanics), we start with a normalized initial two-electron state $|I\rangle$, which is an eigenstate of the unperturbed Hamiltonian $H_1 + H_2$. The interaction U then generates a final state

$$|F_T\rangle = T|I\rangle, \tag{2}$$

where T is the transition operator satisfying the equation $T = U + UG_0T$ and G_0 is the unperturbed two-electron Green function. If one imposes specific boundary conditions, which are characterized by an unperturbed normalized two-electron final state $|F\rangle$, the specific outgoing electron state is the projection

$$|F\rangle\langle F|F_T\rangle = |F\rangle\langle F|T|I\rangle, \tag{3}$$

where $\langle F|T|I\rangle$ is the transition matrix element. The observed reaction cross section is then $|\langle F|T|I\rangle|^2$.

We now proceed to specifying in detail the two-electron states $|I\rangle$ and $|F\rangle$, which are appropriate for the (e,2e) process. The basic ingredients of these two-electron states are one-electron states, which are eigenstates of H_1 and H_2 [cf. Eq. (1)]. For the sake of simplicity and transparency we neglect here spin-orbit coupling, which has been found to be a reasonable approximation for low-Z surfaces (like, e.g., Cu, Fe). The one-electron states are then characterized by energy E, momentum $\vec{k}^{\parallel}$ parallel to the surface, and spin orientation σ with respect to a fixed direction. This direction is arbitrary for nonmagnetic crystals and along the majority spin direction (i.e., opposite to the magnetization direction) for crystals with collinear ferromagnetic structure. The one-electron states can then be expressed as a product of a scalar spatial part $|E,\vec{k}^{\parallel}\rangle^{\sigma}$ and a Pauli spinor $|\sigma\rangle = |\pm\rangle$ [with $|+\rangle = (1,0)$ and $|-\rangle = (0,1)$]. Note that the spatial part is different for spin-up and for spin-down in the case of a ferromagnet, but the same for a nonmagnetic surface system.

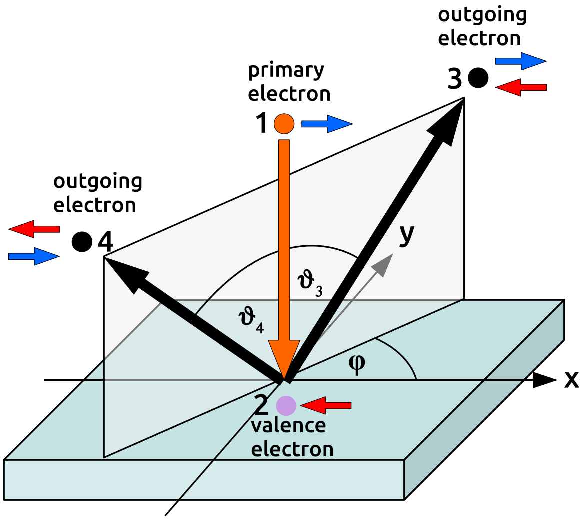

FIG. 1. (Color online) Schematic setup for electron-induced emission of entangled electron pairs from a crystal surface. A primary electron with definite spin and kinetic energy E_1 impinges perpendicularly, i.e., with surface-parallel momentum $\vec{k}_1^{\parallel} = 0$, on the surface and collides with a bound-state valence electron of opposite spin, energy E_2, and parallel momentum $\vec{k}_2^{\parallel}$. Subsequently, the two electrons leave the crystal with energies E_3 and E_4 at polar angles ϑ_3 and ϑ_4, i.e., with surface-parallel momenta $\vec{k}_3^{\parallel} = (k_{3x},k_{3y}) = \sqrt{2E_3}\sin\vartheta_3(\cos\varphi, \sin\varphi)$ and $\vec{k}_4^{\parallel} = -\vec{k}_3^{\parallel}$. The numbers 1 to 4 next to the electron symbols (filled circles) stand for $(E_n, \vec{k}_n^{\parallel})$ with $n = 1$ to 4. The spins of the two outgoing electrons are antiparallel to each other, such that either the electron with $(E_3, \vec{k}_3^{\parallel})$ may have the same spin as the primary electron and the electron with $(E_4, \vec{k}_4^{\parallel})$ the opposite spin (direct process), or vice versa (exchange process). The relative weights of the two processes determine the entanglement of the outgoing two-electron state.

The (e,2e) process is illustrated schematically in Fig. 1. The primary electron is represented by a low energy electron diffraction (LEED) state $|E_1,\vec{k}_1^{\parallel},\sigma_1\rangle$ with energy E_1, surface-parallel momentum $\vec{k}_1^{\parallel}$, and spin orientation σ_1 with respect to an arbitrary but fixed direction. The valence electron state $|E_2,\vec{k}_2^{\parallel},\sigma_2\rangle$ is a bound state with energy E_2, parallel momentum $\vec{k}_2^{\parallel}$, and spin σ_2. The two outgoing electrons are described by two time-reversed LEED states $|E_3,\vec{k}_3^{\parallel},\sigma_3\rangle$ and $|E_4,\vec{k}_4^{\parallel},\sigma_4\rangle$ with energies E_3, E_4 and parallel momenta $\vec{k}_3^{\parallel}$, $\vec{k}_4^{\parallel}$, or equivalently by the corresponding three-dimensional momenta $\vec{k}_3$ and $\vec{k}_4$, which point into the directions of the two detectors. The spins of the outgoing electrons are labeled by σ_3 and σ_4. With energies and parallel momenta of the primary electron and of the two outgoing electrons fixed by boundary conditions, the respective values for the valence electron are dictated by conservation of energy and of parallel momentum (modulo a parallel reciprocal lattice vector):

$$E_1 + E_2 = E_3 + E_4 \quad \text{and} \quad \vec{k}_1^{\parallel} + \vec{k}_2^{\parallel} = \vec{k}_3^{\parallel} + \vec{k}_4^{\parallel}. \tag{4}$$

To make the following more transparent, we write the above four states as $|n,\sigma_n\rangle = |n\rangle|\sigma_n\rangle$ with $n = 1,\ldots,4$, where $|n\rangle$ stands for the spatial part $|E_n,\vec{k}_n^{\parallel}\rangle^{\sigma_n}$, which depends on the spin orientation σ_n in the case of a ferromagnetic system.

The initial two-electron state $|I\rangle$ is an antisymmetrized product of the incoming and valence one-electron states

$$|I\rangle_{\sigma_1\sigma_2} = \frac{1}{\sqrt{2}}(|1,\sigma_1\rangle|2,\sigma_2\rangle - |2,\sigma_2\rangle|1,\sigma_1\rangle). \tag{5}$$

First consider the case that the spins of primary and valence electrons are parallel to each other, i.e., $\sigma_1 = \sigma_2 =: \sigma$. In the absence of spin-orbit coupling, the spins of the two outgoing electrons are the same, i.e., $\sigma_3 = \sigma_4 = \sigma$. The only unperturbed normalized final state, which is subject to the fixed energy-momentum boundary conditions and allows a nonzero transition amplitude, is then the antisymmetrized product

$$|F\rangle^n_{\sigma\sigma} = \frac{1}{\sqrt{2}}(|3,\sigma\rangle|4,\sigma\rangle - |4,\sigma\rangle|3,\sigma\rangle). \tag{6}$$

As is readily seen, the transition amplitude [cf. Eq. (3)] is ${}^{\;n}_{\sigma\sigma}\langle F|T|I\rangle_{\sigma\sigma} =: f_{\sigma\sigma} - g_{\sigma\sigma}$, where $f_{\sigma\sigma}$ and $g_{\sigma\sigma}$ are the direct and exchange matrix elements between the spatial parts $|n\rangle = |E_n,\vec{k}^{\parallel}_n\rangle^{\sigma}$:

$$f_{\sigma\sigma} = \langle 3|\langle 4|T|1\rangle|2\rangle \quad \text{and} \quad g_{\sigma\sigma} = \langle 4|\langle 3|T|1\rangle|2\rangle. \tag{7}$$

The projected state [cf. Eq. (3)] of two parallel-spin outgoing electrons is thus

$$|F\rangle_{\sigma\sigma} = (f_{\sigma\sigma} - g_{\sigma\sigma})|F\rangle^n_{\sigma\sigma} \tag{8}$$

and the observable reaction cross section (intensity) is

$$I_{\sigma\sigma} = {}_{\sigma\sigma}\langle F|F\rangle_{\sigma\sigma}\delta(E)\delta(\vec{k}^{\parallel}) = |f_{\sigma\sigma} - g_{\sigma\sigma}|^2\delta(E)\delta(\vec{k}^{\parallel}), \tag{9}$$

where the δ functions $\delta(E)$ and $\delta(\vec{k}^{\parallel})$ indicate the conservation of energy and parallel momentum [cf. Eq. (4)].

In the case of antiparallel spins $\sigma_1 =: \sigma$ and $\sigma_2 = -\sigma$ of the primary and valence electrons, nonvanishing matrix elements exist for two sets of spins of the two outgoing electrons: (a) the direct matrix element $f_{\sigma\bar{\sigma}}$ if $\sigma_3 = \sigma$ and $\sigma_4 = -\sigma$, and (b) the exchange matrix element $g_{\sigma\bar{\sigma}}$ if $\sigma_3 = -\sigma$ and $\sigma_4 = \sigma$, with $f_{\sigma\bar{\sigma}}$ and $g_{\sigma\bar{\sigma}}$ analogous to $f_{\sigma\sigma}$ and $g_{\sigma\sigma}$ in Eq. (7). The corresponding normalized final states are

$$|F_d\rangle^n_{\sigma\bar{\sigma}} = \frac{1}{\sqrt{2}}(|3,\sigma\rangle|4,-\sigma\rangle - |4,-\sigma\rangle|3,\sigma\rangle) \tag{10a}$$

and

$$|F_e\rangle^n_{\sigma\bar{\sigma}} = \frac{1}{\sqrt{2}}(|3,-\sigma\rangle|4,\sigma\rangle - |4,\sigma\rangle|3,-\sigma\rangle). \tag{10b}$$

Note that these two states are orthogonal to each other. If the outgoing spin set (σ_3,σ_4) is actually fixed (e.g., by means of spin filters in the paths of the two electrons), the corresponding outgoing two-electron state is then either $f_{\sigma\bar{\sigma}}|F_d\rangle^n_{\sigma\bar{\sigma}}$ or $-g_{\sigma\bar{\sigma}}|F_e\rangle^n_{\sigma\bar{\sigma}}$, and the intensity is either $|f_{\sigma\bar{\sigma}}|^2$ or $|g_{\sigma\bar{\sigma}}|^2$. If the set (σ_3,σ_4) is not fixed, i.e., allowed to be either $(\sigma,-\sigma)$ or $(-\sigma,\sigma)$, the outgoing two-electron state $|F\rangle_{\sigma\bar{\sigma}}$ is the projection of the final state $|F_T\rangle = T|I\rangle$ [cf. Eqs. (2) and (4)] on to the subspace spanned by the two orthonormal states $|F_d\rangle^n_{\sigma\bar{\sigma}}$ and $|F_e\rangle^n_{\sigma\bar{\sigma}}$:

$$|F\rangle_{\sigma\bar{\sigma}} := f_{\sigma\bar{\sigma}}|F_d\rangle^n_{\sigma\bar{\sigma}} - g_{\sigma\bar{\sigma}}|F_e\rangle^n_{\sigma\bar{\sigma}}. \tag{11}$$

The reaction cross section for the antiparallel spin case is then

$$I_{\sigma\bar{\sigma}} = {}_{\sigma\bar{\sigma}}\langle F|F\rangle_{\sigma\bar{\sigma}}\delta(E)\delta(\vec{k}^{\parallel}) = (|f_{\sigma\bar{\sigma}}|^2 + |g_{\sigma\bar{\sigma}}|^2)\delta(E)\delta(\vec{k}^{\parallel}). \tag{12}$$

III. ENTANGLEMENT OF THE ELECTRON PAIR AFTER COLLISION

A. Concepts and analytical results

Before dealing with the entanglement of the specific two-electron states, which we obtained in Sec. II, we would like to recall the most pertinent aspects of entanglement of two-electron states in general.

In the case of distinguishable particles, a two-particle state is commonly defined as entangled if it cannot be expressed as a single product of two one-particle states. A naive transfer of this formal definition to the case of two identical (spin 1/2) fermions is however not physically adequate, as has been discussed extensively in the literature ([3,20,29] and references therein). Rather, one should adopt a "physical" definition, according to which a two-particle state is referred to as genuinely entangled if it is not possible to attribute a complete set of properties to both particles individually. Only then there exist quantum correlations which may violate Bell's inequalities or may be used for teleportation. This holds for distinguishable as well as for identical particles. For distinguishable particles, this definition is equivalent to the above formal one. For two electrons, however, it implies that a single Slater determinant, i.e., a single antisymmetrized product of two one-electron states, is not genuinely entangled, whereas it would appear entangled in the sense of not being representable as a single product of one-electron states. A two-electron state $|1,2\rangle$ consisting of a linear combination of linearly independent Slater determinants with expansion coefficients a_k, which satisfy the normalization condition $\sum_k |a_k|^2 = 1$, is genuinely entangled if the number of nonzero coefficients a_k (referred to as the Slater number) is greater than one.

A quantitative measure of the entanglement of $|1,2\rangle$ can hence be introduced as a real positive function of these coefficients a_k. Choosing—in analogy with the case of distinguishable particles—the von Neumann entropy $S_N = -\,\mathrm{tr}[\rho_1 \log_2(\rho_1)]$, where ρ_1 is the one-electron reduced density matrix corresponding to the state $|1,2\rangle$, one obtains [cf., e.g., [3], Eq. (12)]

$$S_N = 1 - \sum_k |a_k|^2 \log_2(|a_k|^2). \tag{13}$$

For a single Slater determinant (with only one coefficient $a_1 = 1$), which according to the above definition is not genuinely entangled, one thus obtains $S_N = 1$, and genuinely entangled states are characterized by $S_N > 1$. It is therefore more appropriate to use as a measure of entanglement the modified entropy

$$S = S_N - 1 = -\sum_k |a_k|^2 \log_2(|a_k|^2). \tag{14}$$

Returning now to the specific two-electron states, which are relevant for (e,2e), we first note that the initial state $|I\rangle$ [cf. Eq. (5)] is just a single Slater determinant. It is therefore not entangled, and according to Eq. (14) it has entropy $S = 0$. The same holds for the final state $|F\rangle_{\sigma\sigma}$ [cf. Eq. (8)] obtained in the case of parallel spins of the two outgoing electrons.

In contrast, the antiparallel-spin final two-electron state $|F\rangle_{\sigma\bar{\sigma}}$ [cf. Eq. (11)] is a linear combination of two antisymmetrized products of two one-electron states. Since in general both coefficients $f_{\sigma\bar{\sigma}}$ and $g_{\sigma\bar{\sigma}}$ are nonzero, it is genuinely entangled (with Slater number 2). In order to calculate its entropy S, we normalize it, replacing $f_{\sigma\bar{\sigma}}$ and $g_{\sigma\bar{\sigma}}$ by

$$\tilde{f} = f_{\sigma\bar{\sigma}}/\sqrt{|f_{\sigma\bar{\sigma}}|^2 + |g_{\sigma\bar{\sigma}}|^2} \tag{15a}$$

and

$$\tilde{g} = g_{\sigma\bar{\sigma}}/\sqrt{|f_{\sigma\bar{\sigma}}|^2 + |g_{\sigma\bar{\sigma}}|^2} \tag{15b}$$

such that $|\tilde{f}|^2 + |\tilde{g}|^2 = 1$. According to Eq. (14) we then obtain

$$S = -|\tilde{f}|^2 \log_2 |\tilde{f}|^2 - |\tilde{g}|^2 \log_2 |\tilde{g}|^2. \tag{16}$$

Due to the absolute squares, S can be expressed in terms of the direct and exchange intensities $|f_{\sigma\bar{\sigma}}|^2$ and $|g_{\sigma\bar{\sigma}}|^2$.

If the direct matrix element $f_{\sigma\bar{\sigma}}$ has some finite value and the exchange matrix element $g_{\sigma\bar{\sigma}}$ is zero, or vice versa, it is obvious from Eqs. (15) and (16) that the entropy S is zero, and according to Eqs. (10) and (11) the two-electron state $|F\rangle_{\sigma\bar{\sigma}}$ consists of a single Slater determinant. The maximal entanglement, which is possible for $|F\rangle_{\sigma\bar{\sigma}}$, is attained if $|f_{\sigma\bar{\sigma}}|^2 = |g_{\sigma\bar{\sigma}}|^2$. One then has $S = \log_2 2 = 1$.

If $f_{\sigma\bar{\sigma}} = g_{\sigma\bar{\sigma}}$, $|F\rangle_{\sigma\bar{\sigma}}$ can be rewritten in the form

$$|F_{\sigma\bar{\sigma}}\rangle = f_{\sigma\bar{\sigma}} \frac{1}{\sqrt{2}}(|3\rangle|4\rangle + |4\rangle|3\rangle)(|\sigma\rangle|{-\sigma}\rangle - |{-\sigma}\rangle|\sigma\rangle), \tag{17}$$

i.e., as a product of a symmetric spatial part and an antisymmetric spin (singlet) part. This is in fact the form of the paradigmatic two-electron state, which was employed in Bohm's version [17] of the Einstein-Podolsky-Rosen paradox [1] and which clearly violates a Bell inequality (cf., e.g., [3,4] and references therein).

In general, $f_{\sigma\bar{\sigma}}$ and $g_{\sigma\bar{\sigma}}$ depend on the specific surface system and the energies and surface-parallel momenta of the primary electron and of the outgoing electrons. They have to be calculated numerically and yield S somewhere between zero and the maximal value 1, as will be illustrated in Sec. III B.

There is however a special configuration which always leads to the maximal entanglement. Consider the coplanar symmetric geometry with normal incidence of the primary electron on to the surface (cf. Fig. 1) and equal energies ($E_3 = E_4$) and polar angles of the two outgoing electrons. If the reaction plane is perpendicular to a mirror plane normal to the surface or if the surface normal is a twofold rotation symmetry axis, symmetry entails $|f_{\sigma\bar{\sigma}}|^2 = |g_{\sigma\bar{\sigma}}|^2$, and hence from Eqs. (15) and (16) $S = \log_2 2 = 1$, which is the maximal entanglement possible for the two-electron state $|F\rangle_{\sigma\bar{\sigma}}$ [Eq. (11)].

The occurrence of this maximal entanglement for antiparallel spins is universal in two respects. First, for a given crystalline surface system, it does—for any chosen primary energy E_1 and subject to energy conservation—not depend on the values of the outgoing electron energies $E_3 = E_4$ and not on the surface-parallel momenta $\vec{k}_3^{\parallel} = -\vec{k}_4^{\parallel}$, i.e., not on the polar angle $\vartheta_3 = \vartheta_4$ between the emission directions and the surface normal. Second, it does not even depend on the choice of a specific surface system.

Our finding of maximal entanglement for all values of the polar angle $\vartheta_3 = \vartheta_4$ and all values of the outgoing electron energies $E_3 = E_4$ is in contrast to the situation in the scattering of two free electrons via Coulomb interaction (cf. [20]), where—in the laboratory system with one electron initially at rest—maximal entanglement is generated only if—for a given primary energy E_1—each of the two outgoing electrons has energy $E_1/2$. This in turn occurs only for the special value 45° of the scattering angle.

So far the cases of parallel and of antiparallel spins have been considered separately. This is realistic for (e,2e) from surfaces if—for valence electron energy E_2 and parallel momentum $\vec{k}_2^{\parallel}$ as determined by the conservation laws Eq. (4)—only valence electrons with one definite spin orientation contribute to the reaction cross section, which is possible first for ferromagnetic surface systems and second by virtue of (e,2e) selection rules [30], even for nonmagnetic systems.

If valence electrons of both spin orientations contribute, the final two-electron state is a mixed state ρ_F described by the sum of the statistical operators corresponding to the two pure states $|F\rangle_{\sigma\sigma}$ [Eq. (8)] and $|F\rangle_{\sigma\bar{\sigma}}$ [Eq. (11)]:

$$\rho_F := |F\rangle_{\sigma\sigma}\langle F|_{\sigma\sigma} + |F\rangle_{\sigma\bar{\sigma}}\langle F|_{\sigma\bar{\sigma}}. \tag{18}$$

An appropriate measure of the entanglement is then the "entropy of formation" $\tilde{S}$ of ρ_F (cf., e.g., [31]). Since the entropy is zero for the case of parallel spins, we obtain

$$\tilde{S} = S I_{\sigma\bar{\sigma}}/(I_{\sigma\bar{\sigma}} + I_{\sigma\sigma}), \tag{19}$$

where S is the entropy for the antiparallel-spin case [Eq. (16)] and $I_{\sigma\bar{\sigma}}$ and $I_{\sigma\sigma}$ are the intensities for antiparallel and parallel spins [cf. Eqs. (9) and (12)], respectively. $\tilde{S}$ is thus generally smaller than S due to the contribution of parallel-spin electrons.

B. Numerical results

In order to obtain quantitative entanglement results for (e,2e) cases more general than the above-discussed antiparallel-spin equal-energy case, numerical calculations are required. To this end we employed a multiple scattering formalism, which has been described in detail in earlier articles ([21,28] and references therein), to calculate the partial spin-dependent intensities $|f_{\sigma\bar{\sigma}}|^2$ and $|g_{\sigma\bar{\sigma}}|^2$ [cf. Eqs. (11) and (12)] and hence pure-state entropy S according to Eqs. (15) and (16) and the mixed-state entropy of formation $\tilde{S}$ according to Eq. (19). An important feature of this formalism is the inclusion of imaginary self-energy corrections, which account for the finite lifetimes of the four quasiparticle states involved and lead to an energy broadening of spectral features.

Since parallel-spin contributions reduce the entanglement, it is desirable to avoid them. This is obviously possible for ferromagnetic surfaces. Selecting valence electron energy regions, in which there are only majority-spin electrons ($\sigma_2 = +$), and using a primary electron beam with opposite spin polarization ($\sigma_1 = -$), the favorable pure antiparallel spin case can be realized experimentally.

As a typical ferromagnetic system we chose the Fe(110) surface, which has been the subject of a previous experimental and theoretical (e,2e) investigation [32]. Specific theoretical model features, in particular quasiparticle potentials and the screening of the Coulomb interaction, were taken to be the same as in [32]. Using these model features, spin-dependent (e,2e) intensity spectra were obtained in good agreement with experimental data [32]. Since our entanglement measure S is a function of partial intensities, it should also be quite realistic.

In Fig. 2 we present (e,2e) results from ferromagnetic Fe(110) obtained for the coplanar symmetric geometry sketched in Fig. 1 with fixed polar and azimuthal emission angles $\vartheta_3 = \vartheta_4$ and $\varphi = \varphi_3 = \varphi_4 + \pi$. The normally incident primary electron has fixed energy $E_1 = 27$ eV, a typical value used in low-energy (e,2e) studies from surfaces. Intensities

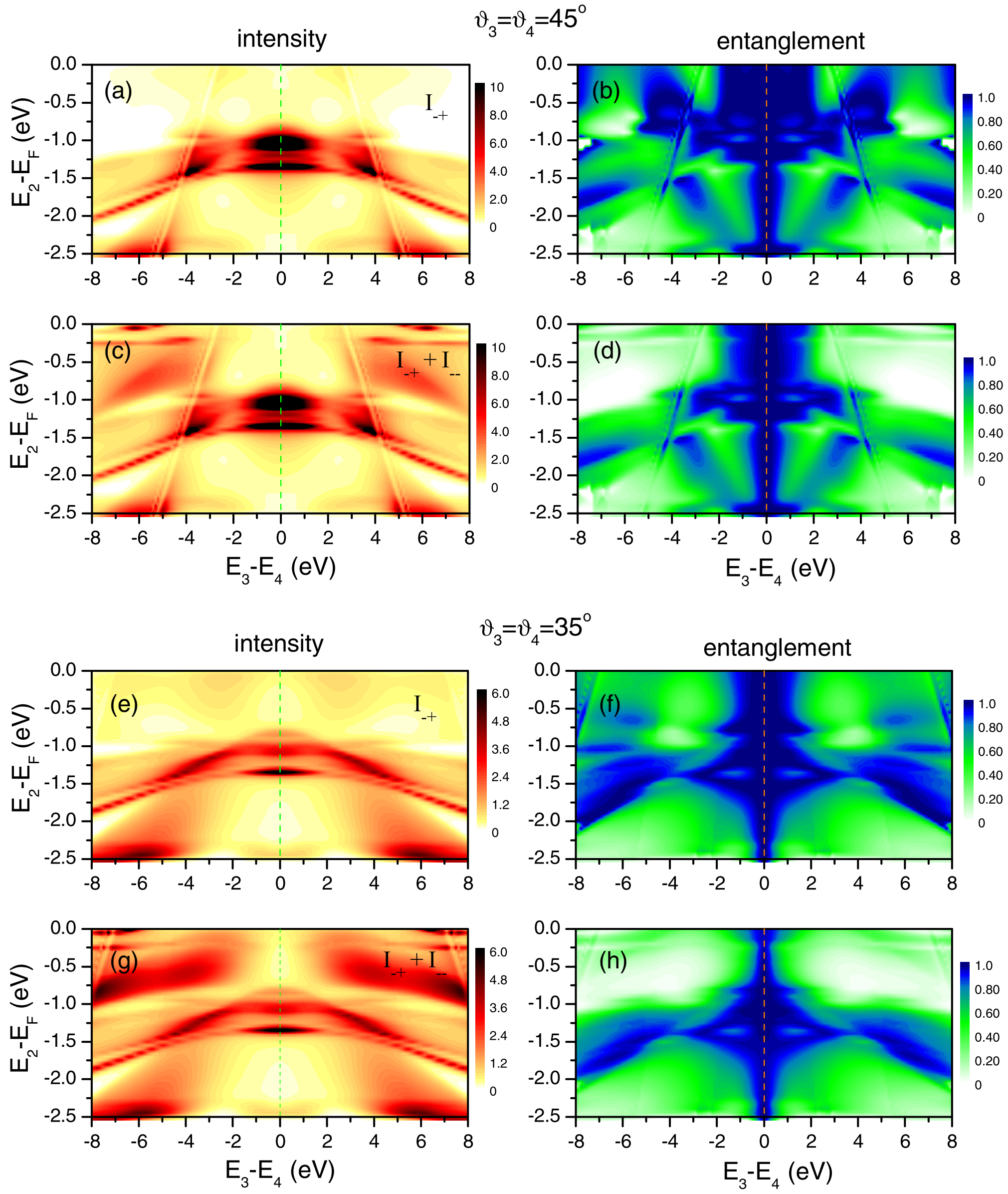

FIG. 2. (Color online) Numerically calculated (e,2e) energy distributions from ferromagnetic Fe(110) for normally incident primary electrons with energy 27 eV and spin $\sigma_1 = -$, i.e., opposite to the spins of the majority valence electrons. The two outgoing electrons have energies E_3 and E_4, equal polar angles $\vartheta_3 = \vartheta_4$, and azimuthal angles $\varphi_3 = 0$ and $\varphi_4 = 180^\circ$. The azimuthal angle φ of the reaction plane (cf. Fig. 1) is 0, with x along the [0,0,1] direction. The vertical axis indicates the valence energy E_2 relative to the Fermi energy E_F, which by virtue of energy conservation [cf. Eq. (4)] is equivalent to the sum energy $E_3 + E_4$ of the outgoing electrons. (a) Antiparallel-spin intensity I_{-+} [cf. Eq. (12)] for polar angles $\vartheta_3 = \vartheta_4 = 45^\circ$. (b) Entropy S [calculated according to Eqs. (15) and (16)]. (c) Total intensity $I_{-+} + I_{--}$, where I_{--} is the parallel-spin intensity [cf. Eq. (9)]. (d) Entropy of formation $\tilde{S}$ [cf. Eq. (19)]. (e) and (f) as (a) and (b) but for $\vartheta_3 = \vartheta_4 = 35^\circ$. (g) and (h) as (c) and (d) but for $\vartheta_3 = \vartheta_4 = 35^\circ$.

and entropies then depend only on the two outgoing electron energies E_3 and E_4. Since the energy sum $E_3 + E_4$ is equal to $E_1 + E_2$ [cf. Eq. (4)], they can equivalently be regarded as functions of the energy difference $E_3 - E_4$ and the valence electron energy $E_2 + \Phi = E_2 - E_F$ relative to the Fermi energy E_F, where Φ is the work function. Furthermore, in our geometry the conservation laws Eq. (4) associate with each pair (E_3, E_4) a unique value of valence electron parallel-momentum $\vec{k}_2^{\parallel} = (k_{2r}, 0)$, where k_{2r} is the component in the reaction plane:

$$k_{2r} = (\sqrt{2E_3} - \sqrt{2E_4})\sin\vartheta \quad \text{with} \quad \vartheta = \vartheta_3 = \vartheta_4. \tag{20}$$

This implies in particular that electrons with $E_3 - E_4 = 0$ originate from collisions with valence electrons with $\vec{k}_2^{\parallel} = (0,0)$, i.e., at the center of the surface Brillouin zone. The presentation of (e,2e) results as functions of $E_3 - E_4$ and $E_2 - E_F$ thus facilitates the association of individual (e,2e) intensity features with features of the underlying $\vec{k}^{\parallel}$-resolved valence electron density of states.

Figure 2(a) shows, for primary electron energy $E_1 = 27$ eV and polar emission angles 45°, the antiparallel-spin cross section I_{-+} [cf. Eq. (12)], i.e., with valence electron spin $\sigma_2 = +$ (parallel to the majority electron spin direction) and

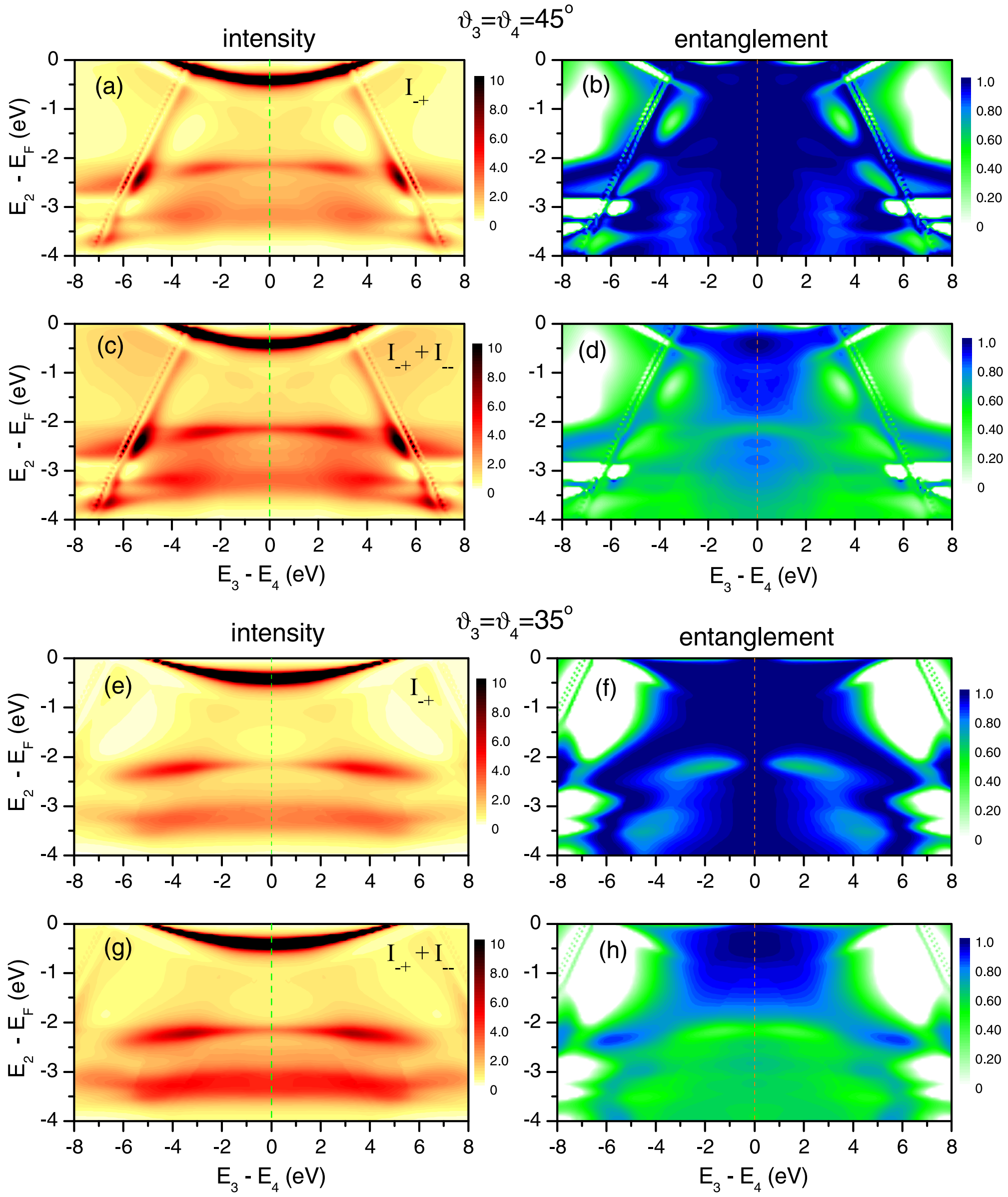

FIG. 3. (Color online) Numerically calculated (e,2e) energy distributions from Cu(111) for normally incident primary electrons with energy 27 eV and spin $\sigma_1 = -$. The two outgoing electrons have energies E_3 and E_4 and equal polar angles $\vartheta_3 = \vartheta_4$. The azimuthal angle φ of the reaction plane (cf. Fig. 1) is 0, with x along the [1, −1,0] direction. The results are displayed in the same way as those in Fig. 2.

primary electron spin $\sigma_1 = -$ (antiparallel to the majority spin direction). Along the dashed vertical line, i.e., for equal energies $E_3 = E_4$ of the outgoing electrons, the salient features are two maxima between valence energies -1 and -1.5 eV. These two maxima reflect the layer-resolved density of states of spin-up valence electrons at $\vec{k}_2^{\parallel} = 0$ (cf. [32]), as one would expect from Eq. (20). Going away from the equal-energy line, i.e., for increasing finite k_{2x}, the two intensity maxima persist, dispersing downward in energy and getting weaker, and two new features appear below -2.3 eV.

The entropy S, which is associated with the intensity I_{-+}, is shown in Fig. 2(b). Along the (dashed) equal-energy line, S reaches the maximally possible value 1, as one expects from our above analytical result. With increasing energy difference S is seen to decrease, but large values are still found near the equal-energy line (e.g., $S = 0.953$ for $|E_3 - E_4| = 0.5$ eV) and in a few regions further out. While the former appear plausible on continuity grounds, the E_2-dependent extent of the large-S stripe around the equal-energy line and the occurrence of the outer large-S regions have no intuitive explanation, but can only be ascribed to complicated multiple scattering processes in the individual electron states affecting the relative weights of the absolute squares of the direct and exchange matrix elements, which determine the entropy [cf. Eq. (16)].

Figures 2(a) and 2(b) show that electron pairs with highest intensity and largest entropy originate from the central region, which is about 0.5 eV wide in valence electron energy and about 2 eV in the difference of the outgoing-electron energies.

If—at energy E_2 and momentum $\vec{k}_2^{\parallel}$—there are also minority-spin electrons in the ferromagnet, which for spin-down primary electrons lead to the (e,2e) intensity I_{--} [cf.

Eq. (9)], the experimentally observable intensity is $I_{-+} + I_{--}$. This total intensity is presented in Fig. 2(c). Comparison with I_{-+} in Fig. 2(a) shows that for equal energies (along the dashed line) there is no parallel-spin contribution. The reason for this is that there exist no contributing minority-spin states (cf. band structure and densities of states shown in [32]). This also holds over the entire energy difference range for valence energies below -1 eV, whereas above -1 eV there is a dominant contribution of I_{--} at larger energy differences.

The corresponding effects on the entanglement of formation $\tilde{S}$ [cf. Eq. (19)] are shown in Fig. 2(d). $\tilde{S}$ is much smaller than S in the regions with significant parallel-spin contribution, while it is almost the same in the remainder of the plot. In particular, for $E_3 = E_4$ the maximal entanglement persists as well as do the large values up to about $|E_3 - E_4| = 1.5$ eV (e.g., $\tilde{S} = 0.94$ for $|E_3 - E_4| = 0.5$ eV).

To demonstrate the existence of strong entanglement for polar angles (of the two outgoing electrons) other than 45°, we show in Figs. 2(e)–2(h) (e,2e) results for ferromagnetic Fe(110) analogous to those in Figs. 2(a)–2(d) but for polar angles $\vartheta_3 = \vartheta_4 = 35^\circ$. As the most important finding we point out that in the central region around the equal-energy line (along which there is of course $S = 1$) there is still high intensity associated with strong entanglement. The same was found in calculations for angles larger than 45°.

In nonmagnetic materials, with no spin polarization of the valence electrons, there is—for all energies and parallel momenta—always an equal number of spin-up and spin-down partners available for collisions with primary electrons of definite spin. So one might expect that for, e.g., spin-down ($\sigma_1 = -$), primary electrons there is, in addition to the antiparallel-spin (e,2e) intensity I_{-+}, always a parallel-spin intensity I_{--} and consequently—according to Eq. (19)—less entanglement. For our coplanar symmetric geometry there are however selection rules [30] which suppress I_{--} (and I_{++}). If, for equal energies of the outgoing electrons, the reaction plane is chosen perpendicular to a mirror plane normal to the surface, the matrix elements $f_{\sigma\sigma}$ and $g_{\sigma\sigma}$ are equal if the relevant valence state has even mirror symmetry. Consequently, $I_{\sigma,\sigma} = 0$ and one has maximal entanglement with entropy $S = 1$.

As a typical nonmagnetic surface we chose Cu(111). Specific theoretical model features, in particular quasiparticle potentials and the screening of the Coulomb interaction, were taken to be the same as in previous (e,2e) work [33].

Results of our (e,2e) calculations are shown in Fig. 3, laid out analogous to Fig. 2. The antiparallel-spin intensity I_{-+} for $\vartheta_3 = \vartheta_4 = 45^\circ$ [Fig. 3(a)] and 35° [Fig. 3(e)] is seen to be dominated by the arched structure, which from valence energy about 0.4 eV below the Fermi energy E_F at $E_3 - E_4 = 0$ disperses upward towards E_F. This structure reflects the *sp*-like Shockley surface state (cf. [34] and references therein). The intensity features below -2 eV originate from the *d*-band region. The entropy S in Figs. 3(b) and 3(f) extends, from the universal maximal value 1 at equal energies, with still large values quite far outward.

The inclusion of the parallel-spin intensity I_{--} is seen [in Figs. 3(c) and 3(g)] to make no difference to the Shockley-derived arched structure. It contributes however substantially to the *d*-band-derived region below -2 eV, in particular also at equal energies. The reason for this different behavior lies in the symmetry of the respective valence states with respect to the mirror plane, which is normal to the reaction plane and normal to the surface. The Shockley state has even symmetry, where $I_{--} = 0$ by virtue of (e,2e) selection rules. In contrast, there are *d* states of even and of odd symmetry. The latter entail nonvanishing I_{--}. The effect on the entanglement is illustrated in Figs. 3(d) and 3(h). In regions with significant contributions of I_{--} it is substantially reduced ($\tilde{S} < S$), while nearly unchanged elsewhere. In particular, strongly entangled electron pairs are emitted with high intensity in the region of the Shockley surface state. Results similar to the ones for $\vartheta_3 = \vartheta_4 = 35^\circ$ and 45° presented in Fig. 3 were obtained for further polar angles between 30° and 60°.

IV. CONCLUDING REMARKS

In the present theoretical work we have explored the spin entanglement of two electrons, which are emitted from a solid surface due to the collision of an incident low-energy electron with a bound valence electron. Analytical calculations revealed that in coplanar symmetric setups the entanglement of two emitted antiparallel-spin electrons with equal energies is always maximal irrespective of their energies and their emission angles and even of the choice of the surface system. For unequal energies of two antiparallel-spin electrons, numerical (e,2e) calculations for the Fe(110) and Cu(111) surface yielded still rather strong entanglement for a fairly wide range of energy and polar angle values.

In (e,2e) experiments using primary electrons with definite spin, there are in general also collisions with valence electrons of the same spin orientation and consequently there are parallel-spin electrons, which are emitted in addition to the antiparallel-spin electrons and lead to a reduction of the entanglement. The avoidance of parallel-spin electrons and hence the preservation of the strong entanglement of the antiparallel-spin electrons is possible for ferromagnets, as we have demonstrated by (e,2e) calculations for the ferromagnetic Fe(110) surface. Due to (e,2e) selection rules, it is even possible for nonmagnetic surfaces, as our results for Cu(111) show.

In view of experimental studies of entanglement creation in (e,2e) we would like to briefly comment on potential modifications of our theoretical results due to energy and angular uncertainties in experimental apparatus. A typical uncertainty of 0.5 eV in the primary electron energy has almost no effect on our intensity and entanglement results. To assess the influence of such uncertainty in the outgoing electron energies, we convoluted the intensities in Figs. 2 and 3 with a Gaussian of 0.5 eV width and calculated the corresponding entanglement of formation. While features in the resulting intensities are noticeably broadened, the entanglement is much less affected. For example, in the high-intensity large-entanglement region obtained for Fe(110) about 1 eV below E_F [cf. Figs. 2(a)–2(d)] the entropy changes for equal energies $E_3 = E_4$ from the maximal value 1 to 0.997 and for $|E_3 - E_4| = 0.5$ eV from 0.953 to 0.954. The effect of an uncertainty of the order of 1 deg in the polar angles of primary and emitted electrons turned out to be minute for both entanglement and intensities.

With regard to comparing our results with results of previous theoretical studies of bipartite entanglement creation by interaction, we note that Refs. [9–16] involve momentum or position entanglement, whereas we focused on spin entanglement. Compared to the spin entanglement results in the scattering of two antiparallel-spin free fermions [20], our results for (e,2e) from surfaces offer the advantage that maximal entanglement is obtained for a range of energies $E_3 = E_4$ (rather than only for $E_3 = E_4 = E_1/2$) and for all scattering angles (rather than only for 45°). The latter feature is due to the fact that the three-dimensional momentum of the two outgoing electrons is—in contrast to the free electron case—not determined by the momenta of the initial electrons, since momentum can be "absorbed" by the crystal. The range of energies $E_3 = E_4$ originates, for a given fixed primary electron energy, via energy conservation from the availability of a range of valence electron energies.

Since (e,2e) from single atoms is sort of intermediate between free electron collisions and (e,2e) from crystal surfaces, one can also expect spin-entangled electron pairs in spin-polarized (e,2e) from atomic targets in the gas phase. While we are not aware of such an entanglement study, we can infer a salient feature from calculated angular intensity distributions in low-energy (e,2e) from H, Na, and Mg atoms [35,36]. In the coplanar symmetric configuration with equal energies of the two electrons, the parallel-spin intensity was found to vanish and the antiparallel-spin intensity to have finite values for all scattering angles. Since vanishing parallel-spin intensity is associated with the direct scattering amplitude f being equal to the exchange scattering amplitude g, the antiparallel-spin pairs are maximally entangled just like those in (e,2e) from surfaces.

ACKNOWLEDGMENT

We are pleased to acknowledge stimulating discussions with J. Kirschner.

---

[1] A. Einstein, B. Podolsky, and N. Rosen, Phys. Rev. **47**, 777 (1935).

[2] E. Schrödinger, Proc. Cambridge Philos. Soc. **31**, 555 (1935); **32**, 446 (1936).

[3] G. C. Ghirardi and L. Marinatto, Phys. Rev. A **70**, 012109 (2004).

[4] J. F. Clauser and A. Shimony, Rep. Prog. Phys. **41**, 1881 (1978).

[5] G. Burkard, J. Phys.: Condens. Matter **19**, 233202 (2007).

[6] M. D. Reid, P. D. Drummond, W. P. Bowen, E. G. Cavalcant, P. K. Lam, H. A. Bachor, U. L. Andersen, and G. Leuchs, Rev. Mod. Phys. **81**, 1727 (2009).

[7] R. Horodecki, P. Horodecki, M. Horodecki, and K. Horodecki, Rev. Mod. Phys. **81**, 865 (2009).

[8] D. J. Wineland, Rev. Mod. Phys. **85**, 1103 (2013).

[9] J. Wang, C. K. Law, and M. C. Chu, Phys. Rev. A **73**, 034302 (2006).

[10] F. Buscemi, P. Bordone, and A. Bertoni, Phys. Rev. A **73**, 052312 (2006).

[11] F. Buscemi, P. Bordone, and A. Bertoni, Phys. Rev. A **75**, 032301 (2007).

[12] N. L. Harshman and G. Hutton, Phys. Rev. A **77**, 042310 (2008)

[13] N. L. Harshman and P. Singh, J. Phys. A: Math. Theor. **41**, 155304 (2008)

[14] R. Weder, Phys. Rev. A **84**, 062320 (2011).

[15] R. Weder, Ann. Phys. **337**, 94 (2013).

[16] M. G. Benedict, J. Kovacs, and A. Czirjak, J. Phys. A: Math. Theor. **45**, 085304 (2012).

[17] D. Bohm, Phys. Rev. **85**, 166 (1952).

[18] J. S. Bell, Physics **1**, 195 (1964).

[19] J. Kessler, *Polarized Electrons* (Springer, Berlin, 1985).

[20] L. Lamata and J. Leon, Phys. Rev. A **73**, 052322 (2006).

[21] R. Feder and H. Gollisch, in *Solid State Photoemission and Related Methods*, edited by W. Schattke and M. A. Van Hove (Wiley-VCH, Weinheim, 2003).

[22] S. Samarin, O. M. Artamonov, A. D. Sergeant, R. Stamps, and J. F. Williams, Phys. Rev. Lett. **97**, 096402 (2006).

[23] F. Giebels, H. Gollisch, R. Feder, F. O. Schumann, C. Winkler, and J. Kirschner, Phys. Rev. B **84**, 165421 (2011).

[24] S. Samarin, O. M. Artamonov, V. N. Petrov, M. Kostylev, L. Pravica, A. Baraban, and J. F. Williams, Phys. Rev. B **84**, 184433 (2011).

[25] Z. Wei, F. O. Schumann, R. S. Dhaka, and J. Kirschner, Phys. Rev. B **85**, 195120 (2012).

[26] F. O. Schumann, C. Winkler, and J. Kirschner, Phys. Rev. B **88**, 085129 (2013).

[27] F. Giebels, H. Gollisch, and R. Feder, Phys. Rev. B **88**, 155422 (2013).

[28] H. Gollisch, N. V. Schwartzenberg, and R. Feder, Phys. Rev. B **74**, 075407 (2006).

[29] J. Schliemann, J. I. Cirac, M. Kus, M. Lewenstein, and D. Loss, Phys. Rev. A **64**, 022303 (2001).

[30] R. Feder and H. Gollisch, Solid State Commun. **119**, 625 (2001).

[31] C. H. Bennett, D. P. DiVincenzo, J. A. Smolin, and W. K. Wootters, Phys. Rev. A **54**, 3824 (1996).

[32] R. Feder and H. Gollisch, in *Correlation Spectroscopy of Surfaces, Thin Films, and Nanostructures*, edited by J. Berakdar and J. Kirschner (Wiley-VCH, Weinheim, 2004).

[33] F. Giebels, H. Gollisch, and R. Feder, J. Phys.: Condens. Matter **21**, 355002 (2009).

[34] H. Gollisch, T. Scheunemann, and R. Feder, Solid State Commun. **117**, 691 (2001).

[35] J. Berakdar, J. S. Briggs, I. Bray, and D. V. Fursa, J. Phys. B: At. Mol. Opt. Phys. **32**, 895 (1999).

[36] G. S. J. Armstrong, J. Colgan, and M. S. Pindzola, Phys. Rev. A **88**, 042713 (2013).